results have been obtained utilizing the integral equation technique (or, equivalently, the boundary element method).

The following observations are in order:

1. The results are closer to the solution of the boundary element (BEM) (or, equivalently, integral equation approach) for fewer boundary layers (i.e., $N_b = 1$) than when the mesh is terminated away from the boundary. This implies that to obtain more accurate results, the mesh must be terminated close to the boundary surface. It is interesting to note that the five-segment boundary element solution provides as accurate a result as a 100-segment finite-difference technique.
2. When the relaxation factor is used as 0.1 and the terminating boundary is close to the surface by two subsection lengths, the results are much closer to the BEM and the results converged in all cases. This is to be expected because in the limit (when the mesh termination coincides with the conductor surfaces) the two techniques coincide.
3. When the mesh termination is far away, the results are of lesser accuracy because of the discretization error in the finite-difference approach. Currently comparison between BEM and this technique is being carried out.
4. Use of a second-order difference (e.g., $hE_{i,j+1} = -1.5 V_{i,j+1} + 2V_{i,j} - 0.5V_{i,j-1}$) for the evaluation of the first derivative in the computation of the charge leads to a faster convergence as shown in Table 2. Again the results are most accurate when the mesh is terminated closer to the boundary.

4. CONCLUSION

The proposed method, a hybrid of differential and integral equation techniques, is quite efficient (as only two layers of discretized cells are required) and accurate (as the radiation condition becomes numerically exact). The solution procedure is fast as the system matrix is still very sparse. An interesting feature of this method is that results are more accurate when the mesh is terminated closer to the boundary.

TABLE 1 Value of Capacitance for the Proposed Hybrid Technique

	N_a				
N_b	5	10	25	50	100
1	23.15	23.98	24.44	24.56	24.62
2	22.41	23.61	24.31	24.51	24.59
5	21.36	22.96	24.09	24.39	24.54
10	20.84	22.46	23.78	24.26	24.49
20	20.59	22.13	23.50	24.09	24.40
50	20.48	21.93	23.23	23.86	24.26
100	20.48	21.89	23.16	23.73	24.15
200	20.48	21.90	23.10	23.69	24.07
BEM	24.61	24.65	24.66	24.66	24.66

TABLE 2 Value of Capacitance for the New Approach Utilizing a Second-Order Approximation for the Derivative

N_a	5	10
N_b	C_2	C_2
2	23.32	24.07
5	22.65	23.66
10	22.31	23.55

This method can be generalized for the case of the inhomogeneous Green's function for nonlinear media, for static and dynamic fields.

REFERENCES

1. M. A. Celia and W. G. Gray, *Numerical Methods for Differential Equations—Fundamental Concepts for Scientific and Engineering Applications*, Prentice Hall, Englewood Cliffs, NJ, 1992.
2. K. K. Mei, R. Pous, Z. Chen, and Y. Liu, "Measured Equation of Invariance: A New Concept in Field Computation," in *IEEE Ant. Prop. Symp. & URSI Radio Science Meeting*, Chicago, IL, 1992.
3. R. F. Harrington, *Field Computation by Moment of Methods*, IEEE Press, New York, 1967.

Received 11-9-94

Microwave and Optical Technology Letters, 8/6, 319–321

CCC 0895-2477/95

TUNABLE RING RESONATOR FILTER FOR OFDM TRANSMISSION SYSTEMS

C. Vázquez and F. Hernández-Gil
Telefónica Investigación y División de Optoelectrónica Desarrollo
Emilio Vargas 6
Madrid 28043, Spain

M. López-Amo
Dpto. Tecnología Fotónica
ETSI de Telecomunicación
Ciudad Universitaria
Madrid 28040, Spain

KEY TERMS

Integrated optics, optical demultiplexers, receivers

ABSTRACT

A novel tunable filter is theoretically demonstrated. It is based on a ring resonator with an amplifier and a noise filter in the loop. This optoelectronic device has potential as a high-sensitivity receiver and as a tunable demultiplexer in OFDM transmission systems. © 1995 John Wiley & Sons, Inc.

INTRODUCTION

Integrated optical resonators have great potential for tunable filters and receivers in optical frequency-division-multiplexing (OFDM) transmission systems [1]. These dense FDM systems make possible CATV distribution of many video channels to each subscriber's home.

A ring resonator with a noise filter and a semiconductor optical amplifier in the loop is presented. The amplifier tailors the round-trip optical loss allowing design flexibility [2], finesse enhancement [3], and relaxed tolerances on the directional coupler that closes the loop. The grating-folded directional coupler filter [4] that combines two identical Bragg reflection gratings on the output arms of a 3-dB coupler provides the desired bandpass response to filter the ASE (amplified spontaneous emission) generated by the amplifier. The presence of the filter within the loop allows only one resonant frequency [5].

This novel photonic circuit has various applications, such as high-sensitivity receivers with a net gain, tunable demultiplexers, and routers in OFDM transmission systems.

DESCRIPTION OF THE PHOTONIC CIRCUIT

The novel configuration of the optical filter is shown in Figure 1. The device diverts one of N input frequencies into

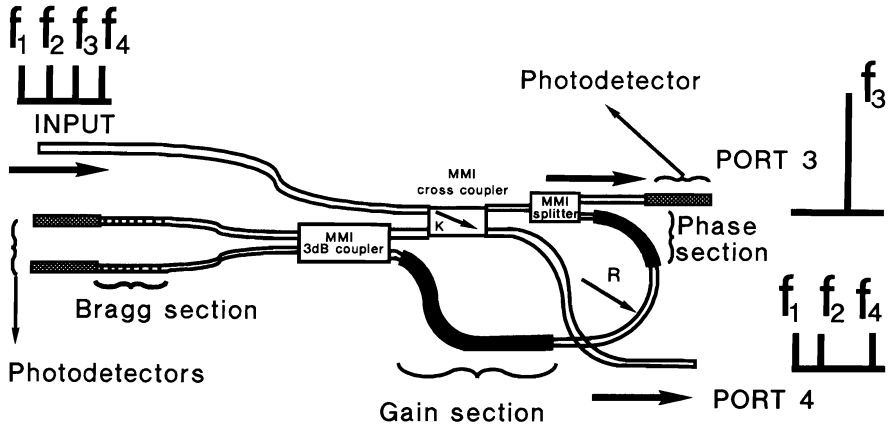

Figure 1 Basic configurations of the proposed optical filter

port 3, and the remaining $N-1$ frequencies are coupled into port 4.

The ring resonator achieves the narrow-band channels of the OFDM systems. The presence of the grating filter allows only one resonant frequency, to avoid unwanted reflection back to the amplifier and the reduction of the power noise of the device. To do so, it must be placed after the amplifier. To achieve lower side-lobe amplitudes in the adjacent channels, a compromise between the FSR of the loop and the full width at half maximum (FWHM) of the transmissive Bragg filter must be established. The Bragg grating must be designed in such a way that the minimum number of resonant frequencies of the loop were within the FWHM. On the other hand, there is also a compromise between the FWHM and the loss of the filter.

The filter tuning is done in two stages as in three-section DBR lasers. The coarse tuning involves the selection of a given spectral period of the resonant loop. To do so, the Bragg filter central frequency is tuned by forward injecting in the Bragg gratings (see Figure 1); tuning ranges of 10 nm can be obtained. The second step involves the tuning of the resonant frequency inside the selected FSR of the loop. This can be achieved by injecting into the phase section.

SPECIFIC DESIGN

The passive backbone waveguide is a 2-μm-wide buried structure with a 0.3-μm-thick $1.3-Q$ InGaAsP layer (λ_{PL} = 1.3 μm, photoluminescence wavelength). The first goal is to keep the loop length as short as possible, so that there will be fewer performance constraints.

A short radius of curvature of 150 μm can be used due to the buried waveguide's large confinement. The estimated minimum bend radius $R > 1.5R_{\text{cutoff}}$ achieves low loss.

The coupler that closes the loop must satisfy the requirement that only a small amount of the incoming power recirculates ($k \to 1$, see Figure 1), to provide a better extinction ratio between adjacent channels. To achieve a more compact device, a cross MMI coupler 5.4 μm wide and 66 μm long is selected. It is shorter than a usual MMI coupler (calculated with the predictions of the self-imaging in multimode waveguide theory) and it is designed with a modal analysis. It has 0.3-μm offset at the input/output waveguides to achieve a gap of 2 μm (to overcome possible lithography limitations in the fabrication process). The selection of a cross coupler instead of a bar one implies a crossover (see Figure 1) between the output waveguides, which has been designed with an angle $> 60°$ to avoid losses. The MMI splitter [6] to extract the resonant frequency is 49 μm long and 6 μm wide.

The 3-dB coupler of the transmissive Bragg filter is a 193-μm-long MMI coupler 6 μm wide, with input/output waveguides with the subsequent offset to take into account the shift of the mode along the bends.

The amplifier and photodetectors consists of six compressively strained InGaAs/InGaAsP quantum wells grown on top of the backbone waveguide, formed in a buried heterostructure. The amplifier is 700 μm long to achieve gains as high as 20 dB in case the losses in the loop were greater than expected. This is the maximum possible length (corresponding to $\frac{3}{4}$ of the loop), considering the existence of the phase section (≥ 100 μm to allow the tuning through all the FSR). With the previous dimensions, the loop length would be 1936 μm, which means a FSR of 0.384 nm (43.45 GHz, higher than the best results reported up to now [1]). The waveguide photodetectors are 200 μm long. Those at the end of the Bragg gratings avoid unwanted reflections. Another photodetector can be equally placed at port 3, in case the device is used as a receiver.

In our design, FWHM $\leq$ 3FSR, for obtaining amplitude side lobes lower than 1 dB in the adjacent channels when $k \to 1$. Obtaining a tolerable level of losses after injecting in the grating to achieve the desired tuning range was also taken into account. So the Bragg grating parameters are L_B = 760 μm, k_B = 32 cm^{-1}, which imply FWHM = 1.052 nm and a maximum transmittivity of 0.305 (−5.16 dB) for the higher injection level considered (α_B = 40 cm^{-1}). L_B, k_B, and α_B denote the length, the coupling coefficient, and the distributed loss coefficient of each Bragg reflector, respectively.

Figure 2 shows both outputs of the novel filter for the previous parameters. It can be seen that depending on the value of the loop gain (G_{loop}), the resonant frequency can be rejected or amplified at port 4. The simulation of the device is based on the equations of an amplified ring resonator [3], but considering the transfer function of the transmissive Bragg filter within the loop. The delays derived from the propagation through the MMI sections and the effective length of the Bragg gratings were taken into account in the loop length. The general features of this device (for the parameters of Figure 2 with G_{loop} = 1.188) are adjacent-channel side-lobe amplitudes lower than 1 dB (for $\alpha_B \geq 4$ cm^{-1}), a tunable range of 10 nm, FWHM_4 = 5.0 MHz, and FWHM_3 = 75 MHz, where the subscripts 3 and 4 are related to the corresponding ports (see Figure 1). There is a net gain

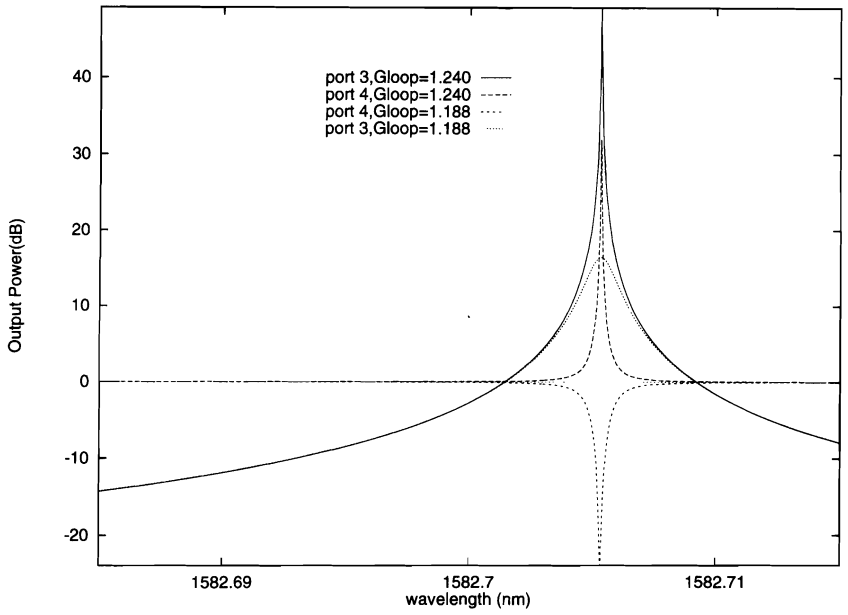

Figure 2 Output optical power (dB). The parameters of the device are Bragg section: $L_B = 760\ \mu m$, $\alpha_B = 5\ cm^{-1}$, $\Lambda_B = 245$ nm (pitch Bragg grating), $n_B = 3.23$. Loop section: $L_{loop} = 1942.245\ \mu m$, $n_P = n_G = 3.23$ (n_B, n_P, and n_G denote the model effective indexes of the Bragg, phase, and gain sections, respectively

of 16 dB at the resonant frequency at port 3, and a low loss of 0.645 dB appears at the other frequencies at port 4 ($(1 - k)\gamma$, where γ denotes the insertion loss of the coupler that closes the loop). The rejection ratio at port 4 is better than 20 dB (optical). A SNR better than 60 dB is obtained when considering the dominant source-induced phase noise for input power (P_0) higher than about -62 dBm. For lower values of P_0, the dominant term is the spontaneous-spontaneous beat noise due to the ASE of the optical amplifier. This is improved with the Bragg filter within the loop [7].

In conclusion, we have theoretically demonstrated a novel tunable filter. Its main advantages are the large number (16,649) of narrow-band (75-MHz) channels and the possibility to tailor the filter response. Other very important advantages that can be achieved with this structure are low loss, net gain of 16 dB in the selected channel, low fabrication tolerances, cross talk < 20 dB and compact size ($1732 \times 425\ \mu m$).

ACKNOWLEDGMENT

The contribution of A. Ferreras to the preparation of this article and the encouragement from Dr. Mustieles are gratefully acknowledged. This work was supported by a grant from the Spanish Ministry of Education and Science. M. López-Amo acknowledges the support of the Spanish CICYT (TIC92-52-CO2).

REFERENCES

1. Kazuhiro Oda, Norio Takato, and Hiromu Toba, "A Wide-FSR Waveguide Double-Ring Resonator for Optical FDM Transmission Systems," *J. Lightwave Technol.*, Vol. 9, No. 6, June 1991, pp. 728–736.
2. M. C. Vázquez, B. Vizoso, M. López-Amo, and M. A. Muriel, "Single and Double Amplified Recirculating Optical Delay Lines as Fiber-Optic Filters," *Electron. Lett.*, Vol. 28, May 1992, pp. 1017–1019.
3. Haruo Okamura and Katsumi Iwatsuki, "A Finesse-Enhanced Er-Doped-Fiber Ring Resonator," *J. Lightwave Technol.*, Vol. 9, No. 11, Nov. 1991, pp. 1554–1560.
4. R. C. Alferness, L. L. Buhl, U. Koren, T. L. Koch, I. Kim, B. I. Miller, M. A. Newkirk, M. G. Young, R. P. Gnall, F. Hernández-Gil, H. M. Presby, G. Raybon, and C. A. Burrus, "Integrated MQW Optical Amplifier/Noise-Filter/Photodetector Photonic Circuit," *IEEE Photon. Technol. Lett.*, Vol. PTL-5, No. 12, Dec. 1993, pp. 1401–1403.
5. J. Capmany, R. I. Laming, and D. N. Payne, "Novel High Selective and Tunable Optical Bandpass Filter Using a Fibre Grating and a Fabry-Perot," *Microwave Opti. Technol. Lett.*, Vol. 7, No. 11, Aug. 1994, pp. 499–501.
6. A Ferreras, F. Rodríguez, E. Gómez-Salas, J. L. de Miguel, and F. Hernández-Gil, "Useful Formulas for Multimode Interference Power Splitter/Combiner Design," *IEEE Photon. Technol. Lett.*, No. 10, Oct. 1993, pp. 1224–1227.
7. J. T. Kringlebotn and K. Blotekjaer, "Noise Analysis of an Amplified Fiber-Optic Recirculating-Ring Delay Line," *J. Lightwave Technol.*, Vol. 12, No. 3, March 1994, pp. 573–582.

Received 9-27-94; revised 11-23-94

Microwave and Optical Technology Letters, 8/6, 321–323

CCC 0895-2477/95

CORRECTION TO "CONFORMAL ABSORBING BOUNDARY CONDITIONS FOR THE VECTOR WAVE EQUATION"

A. Chatterjee and J. L. Volakis
Radiation Laboratory
Department of Electrical Engineering and Computer Science
University of Michigan
Ann Arbor, Michigan 48109

In the above paper [1], the second identity after Eq. (13) was derived incorrectly. The incorrect identity was

$$\hat{\mathbf{n}} \times \nabla \times (\hat{\mathbf{n}} \times \nabla \times \mathbf{E}) = \nabla \times \{\hat{\mathbf{n}}(\nabla \times \mathbf{E})_n\} - k_0^2 \mathbf{E}_t + \Delta\kappa\ \hat{\mathbf{n}} \times \nabla \times \mathbf{E},$$